Simple Conduction Model for Theoretical Steady-State Heat Pipe Performance

K. H. SUN* AND C. L. TIEN †
University of California, Berkeley, Calif.

An analytical model is established for the steady-state thermal performance of single component heat pipes. By considering the interaction of axial heat conduction through the wall with various heat-transfer modes inside and outside the heat pipe, the analysis leads to the prediction of saturated vapor temperature, the axial wall temperature and mass flow distributions along the heat pipe. The thermal performance of a heat pipe is shown to be dependent upon two dimensionless parameters: the Biot number with respect to the wick and a parameter that characterizes the relative contributions of radial conduction through the wick and axial conduction through the pipe wall. The predictions are compared and discussed with existing experimental results.

Nomenclature

Bi = Biot number with respect to wick, defined in Eq. (7)
B_λ, B_0 = Biot numbers with respect to wick for the source and sink regions, respectively, defined by Eq. (A11)
C_{Pi} = specific heat of the liquid-wick matrix
D_0 = outer diameter of the heat pipe
D_i = inner diameter of the heat pipe
D_v = diameter of the vapor core inside the heat pipe
h = heat-transfer coefficient between the pipe wall and ambient
h_{fg} = latent heat of vaporization and condensation
h_λ, h_0 = heat-transfer coefficients in the source and sink regions, respectively
k_i, k_w = thermal conductivity of liquid-wick matrix and pipe wall, respectively
L = total length of heat pipe
L_e, L_a, L_c = length of the heat input, adiabatic and heat output sections, respectively
M = dimensionless parameter, defined in Eq. (4)
m = axial mass flow rate
$\bar{m}$ = dimensionless axial mass flow rate, defined by Eqs. (15, 17, 19, A4, A5 and A6)
Q = rate of heat input to the heat pipe
q = heat flux per unit area
T_0 = ambient sink temperature
T_s = temperature of saturated vapor
T_w = temperature of pipe wall
T_{w1} = wall temperature at the junction of heat input and adiabatic sections
T_{w2} = wall temperature at the junction of heat output and adiabatic sections
$\bar{T}_{wc}$ = observed mean wall temperature at the heat output section
T_λ = temperature of the warm surroundings or the source
t_i, t_w = thickness of wick and wall, respectively
x, y, z = axial coordinate for the heat input, adiabatic and heat output sections, respectively
β = dimensionless length coordinate for the adiabatic section, defined as y/L
β_a = dimensionless length of the adiabatic section, defined as L_a/L
η = dimensionless length coordinate for the heat input section, defined as x/L
η_e = dimensionless length of the heat input section, defined as L_e/L
θ_s = dimensionless saturated vapor temperature, defined by Eq. (A8)
θ_0 = dimensionless saturated vapor temperature, defined in Eq. (7)
θ_1 = dimensionless wall temperature at the junction of heat input and adiabatic sections, defined in Eqs. (4) and (A9)
θ_2 = dimensionless wall temperature at the junction of heat output and adiabatic sections, defined in Eqs. (7) and (A10)
θ_e = dimensionless wall temperature at the heat input section, defined in Eqs. (4) and (A1)
θ_c = dimensionless wall temperature at the heat output section, defined in Eqs. (7) and (A3)
θ_a = dimensionless wall temperature at the adiabatic section, defined in Eqs. (11) and (A2)
ξ = dimensionless length coordinate for the heat output section, defined as z/L
ξ_c = dimensionless length of the heat output section, defined as L_c/L

Subscripts
i = refers to wick (exception D_i)
w = refers to pipe wall
e = refers to heat input section
a = refers to adiabatic section
c = refers to heat output section

Received November 18, 1971; revision received February 10, 1972. Supported by National Science Foundation through Grant NSF GK-11548.
Index category: Thermophysics and Thermochemistry.
* Research Assistant in Mechanical Engineering.
† Professor of Mechanical Engineering. Associate Fellow AIAA.

Introduction

SUCCESSFUL heat pipe design requires a good knowledge of the heat-pipe thermal performance under prescribed ambient conditions and specific heat loads. One common criterion has been based on the exterior wall temperature drop from evaporator to condenser. The apparent thermal conductivity or the thermal effectiveness is high when this temperature drop is small. It is generally accepted that this temperature drop is the sum of the temperature drops across the wick-wall matrix in the evaporator and condenser sections.[1] Axial heat conduction through the pipe wall has been neglected in all existing analyses, except in some recent studies of gas-controlled heat pipes.[2] Considering the over-all thermal performance, however, axial wall conduction might become an important mode of energy transfer as it interacts in a direct manner with various other modes in a heat pipe. Indeed, it is shown in this paper that axial wall conduction may play a significant role in steady-state heat pipe performance.

In the present paper, an analytical model is developed by taking into account the interactions of the axial heat conduction through the heat pipe wall with various transport processes inside and outside of the heat pipe. It is shown that predictions can be made through this analytical model on the thermal performance of a heat pipe, such as the saturated vapor temperature and pressure, the wall temperature profile and the axial mass flow distribution inside the heat pipe.

General Consideration

It is essential in the present analysis first to have a correct understanding of the conventional terms, evaporator and condenser, that are generally used to identify the sections of a heat pipe where heat is added and rejected. These terms are somewhat misleading in the sense that the regions where vaporization and condensation processes take place are not necessarily equivalent to the sections of heat input and output. This is illustrated in Fig. 1 which shows that the region where vaporization process occurs is longer than the heat input section and the region where condensation process occurs can be longer (Fig. 1a) or shorter (Fig. 1b) than the heat output section. It is thus more appropriate to have the conventional "evaporator" and "condenser" named respectively as the "heat input section" and "heat output section" while the regions where vaporization and condensation occur named as the "effective evaporator" and "effective condenser." For heat pipes with an adiabatic (i.e. insulated) section, there exists a near-isothermal region for a long adiabatic section (Fig. 1a), while a short adiabatic section may contain no isothermal region at all.

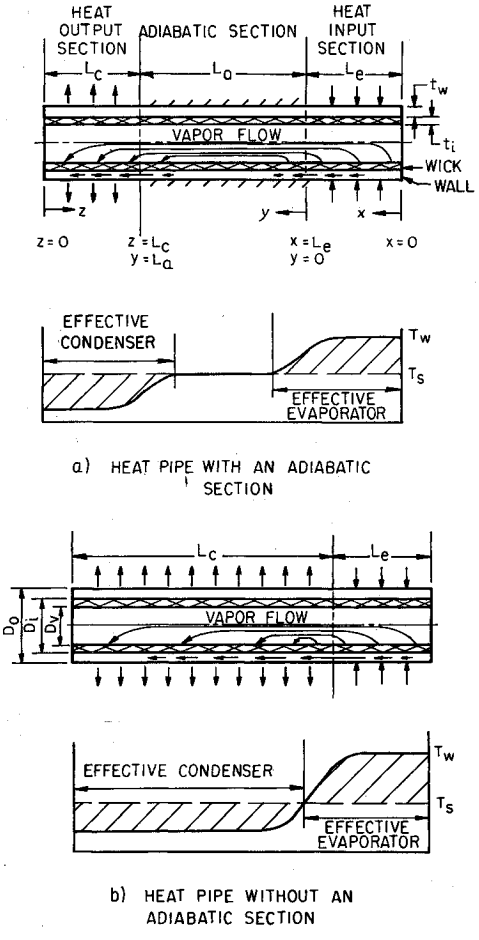

Fig. 1 Axial wall temperature variation along heat pipes.

The present analysis is based on a number of physical assumptions. The heat pipe is assumed to contain only one fluid and is operating under steady-state conditions. This means that the vapor region is near isothermal, and the total energy input and output are equal. The wick is assumed to be fully saturated with the working liquid and convection inside the wick is negligible. The wick-liquid matrix can thus be treated as a homogeneous body with an effective thermal conductivity. The energy transferred through the wick is simply by conduction, and vaporization and condensation take place only at the wick-vapor interface. Convection effects on the temperature variations in the vapor space and in the wick-liquid matrix is to be neglected. In the vapor space, the small variations in pressure as well as its corresponding vapor saturation temperature are indeed negligible, and the vapor zone merely serves as a mass flow passage. The effect of convection in the wick on temperature variations along the pipe wall, however, deserves careful consideration.

The relative importance of convection in the wick can be assessed by comparing the convection contribution with that by conduction. Considering a differential element ΔL of the wick, the ratio of the heat flow due to the enthalpy change in the axial direction to that due to conduction in the radial direction can be expressed as

$$N \equiv \frac{qC_{Pi}\Delta L(T_s - T_w)/h_{fg}}{(T_s - T_w)k_i\Delta L/t_i} = \frac{qC_{Pi}t_i}{h_{fg}k_i} \tag{1}$$

By substituting appropriate values into Eq. (1), N is found to vary from zero to 10^{-3} for high-temperature (i.e. molten metal) heat pipes, to 10^{-2} for water or organic-liquid heat pipes operating at medium temperature ranges, and to 10^{-1} for cryogenic heat pipes. On the basis of these values, it is justified to neglect convection except in some cases of cryogenic heat pipes.

Finally, it is assumed that there exist only axial temperature variations along the wall. This requires that the radial temperature variation inside the wick and outside the heat pipe are much larger than that in the wall. The assumption can be characterized in terms of two dimensionless parameters. The Biot number with respect to the wall, $B \equiv (hD_0/2k_w)\ln(D_0/D_i)$, characterizes the relative magnitude of convection or radiation through the ambient to radial conduction through the wall. The other parameter, $P \equiv [k_i \ln(D_0/D_i)]/[k_w \ln(D_i/D_v)]$, compares radial conduction through the wick against that through the wall. For $B \ll 1$ and $P \ll 1$, the pipe wall can be treated as a fin with only axial temperature variations. For heat pipes with comparable wick and wall thicknesses, $P \ll 1$ also implies the axial conduction through the wick is negligible as compared to that through the wall. Among the existing heat pipes, this assumption is generally true, except for some molten-metal heat pipes.

In short, under the above assumptions, heat transfer is decoupled from fluid flow in the wick. There is axial heat conduction along the pipe wall and radial heat conduction through the wick. The vapor region is in a saturated condition with a uniform temperature throughout, and condensation and vaporization take place only at the wick-vapor interface. These assumptions are very reasonable for medium- and low-temperature heat pipes. For those heat pipes equipped with artery wicks, the "decoupling" assumption is particularly true.[3]

Analysis

Governing Equations and Boundary Conditions

The heat pipe operates generally with the heat input section under the condition of uniform heat addition or placed in a warm surrounding, while leaving the heat output section in a cold ambient. Since the different heat source conditions do not alter the basic nature of the heat pipe performance analysis, only the case of uniform heat addition will be treated in detail. The other case can be treated in a similar manner (see Appendix). The physical system under consideration is a long cylindrical heat pipe with uniform heat addition to the heat input section and negligible heat loss at the ends. Heat conduction equations are first set up for the three (heat input, adiabatic, and heat output) sections with the condition of temperature and heat flux continuity prescribed at their junctions. The coordinate system is given in Fig. 1a.

Based on the cylindrical differential elements, dx, dy, and dz, in each heat pipe section, simple heat balance consideration leads to the following governing equations and boundary conditions in dimensionless forms: for the heat input section, $0 \leqq x \leqq L_e$

$$\theta_e''(\eta) - M^2\theta_e(\eta) + M^2 = 0 \tag{2}$$

$$\theta_e'(0) = 0, \qquad \theta_e(\eta_e) = \theta_1 \tag{3}$$

where

$$\eta \equiv x/L, \quad \eta_e \equiv L_e/L, \quad M \equiv \left[\frac{8k_l L^2}{k_w(D_0^2 - D_i^2)\ln D_i/D_{vL}}\right]^{1/2} \tag{4}$$

$$\theta_e(\eta) \equiv \frac{T_{we}(x) - T_s}{(Q/2\pi L_e k_l)\ln(D_i/D_v)}, \quad \theta_1 \equiv \frac{T_{w1} - T_s}{(Q/2\pi L_e k_l)\ln(D_i/D_v)}$$

for the heat output section, $0 \leqq z \leqq L_c$

$$\theta_c''(\xi) - M^2(1+Bi)\theta_c(\xi) + M^2 Bi\theta_0 = 0 \tag{5}$$

$$\theta_c'(0) = 0, \qquad \theta_c(\xi_c) = \theta_2 \tag{6}$$

where

$$\xi \equiv z/L, \quad \xi_c \equiv L_c/L, \quad Bi \equiv (hD_0/2k_l)\ln(D_i/D_v)$$

$$\theta_c(\xi) \equiv \frac{T_{wc}(z) - T_s}{(Q/2\pi L_e k_l)\ln(D_i/D_v)}$$

$$\theta_0 \equiv \frac{T_0 - T_s}{(Q/2\pi L_e k_l)\ln(D_i/D_v)}, \quad \theta_2 \equiv \frac{T_{w2} - T_s}{(Q/2\pi L_e k_l)\ln(D_i/D_v)} \tag{7}$$

and for the adiabatic section, $0 \leqq y \leqq L_a$

$$\theta_a''(\beta) - M^2\theta_a(\beta) = 0 \tag{8}$$

$$\theta_a(0) = \theta_1, \qquad \theta_a(\beta_a) = \theta_2 \tag{9}$$

$$\theta_a'(0) = \theta_e'(\eta_e), \qquad \theta_a'(\beta_a) + \theta_c'(\xi_c) = 0 \tag{10}$$

where

$$\beta = y/L, \quad \beta_a = L_a/L, \quad \theta_a(\beta) \equiv \frac{T_{wa}(y) - T_s}{(Q/2\pi L_e k_l)\ln(D_i/D_v)} \tag{11}$$

The wall temperature at the junction of heat input and adiabatic sections T_{w1} and at the junction of heat output and adiabatic section T_{w2} are not given, but they will be eliminated through the relations of temperature and heat flux continuities at the junctions. The boundary conditions given above provide sufficient and necessary conditions to solve the dimensionless wall temperatures θ_e, θ_a, and θ_c. The saturated vapor temperature T_s, however, is still an unknown. The fact that T_s must also be determined requires one more equation. This is provided by an enclosure condition.

Enclosure Condition

The enclosure condition is based on the fact that in steady state there are no energy and mass accumulations, the vapor temperature will adjust according to the heat input and ambient conditions, so that the condensing mass rate is equal to the evaporating mass rate, and all the heat input is rejected to the ambient. The energy conservation of a heat pipe in steady state can be expressed by the well-known relation

$$Q = \int_0^{L_c} h[T_{wc}(z) - T_0]\pi D_0\, dz \tag{12}$$

Noting that T_s is constant and assuming that h does not vary appreciably along the heat pipe, Eq. (12) can be written in the dimensionless form

$$\int_0^{\xi_c} \theta_c(\xi)\, d\xi = \eta_e/Bi + \theta_0\,\xi_c \tag{13}$$

The axial mass flow is directly related to radial conduction through wick since vaporization and condensation processes only occur at the wick-vapor interface. By considering the heat input and output, and the energy required for vaporization and condensation, along with axial conduction through the wall, it can be shown that the zero net mass flow and heat flow criteria for the heat pipe enclosure are mutually dependent on each other. This is illustrated graphically in Fig. 1, that the shaded area above the T_s line is equal to the shaded area underneath it.

With the enclosure condition given in Eq. (13), along with the governing equations and boundary conditions, the saturated vapor temperature T_s can be determined.

Solutions

Solutions for the temperature and mass flow distributions in each section can be obtained through simple mathematical manipulations. They are

for $0 \leqq \eta \leqq \eta_e$

$$\theta_e(\eta) = 1 - (1-\theta_1)\cosh M\eta/\cosh M\eta_e \tag{14}$$

$$m(x) = \frac{1}{h_{fg}}\int_0^x 2\pi k_l \frac{T_{we}(x) - T_s}{\ln(D_i/D_v)}\, dx = \frac{QL}{h_{fg}L_e}\int_0^\eta \theta_e(\eta)\, d\eta$$

or

$$\bar{m}(\eta) \equiv \frac{m(x)}{Q/h_{fg}} = \frac{1}{\eta_e}\left[\eta + (\theta_1 - 1)\frac{\sinh M\eta}{M\cosh M\eta_e}\right] \tag{15}$$

for $0 \leqq \xi \leqq \xi_c$

$$\theta_c(\xi) = \frac{Bi\theta_0}{1+Bi} + \left(\theta_2 - \frac{Bi\theta_0}{1+Bi}\right)\frac{\cosh M(1+Bi)^{1/2}\xi}{\cosh M(1+Bi)^{1/2}\xi_c} \tag{16}$$

$$\bar{m}(\xi) \equiv \frac{m(z)}{Q/h_{fg}} = -\frac{L}{L_e}\int_0^\xi \theta_c(\xi)\, d\xi = -$$

$$\frac{1}{\eta_e}\left[\frac{Bi\theta_0\,\xi}{1+Bi} + \frac{[\theta_2 - Bi\theta_0/(1+Bi)]\sinh M(1+Bi)^{1/2}\xi}{M(1+Bi)^{1/2}\cosh M(1+Bi)^{1/2}\xi_c}\right] \tag{17}$$

and for $0 \leqq \beta \leqq \beta_a$

$$\theta_a(\beta) = \theta_1\cosh M\beta + (\theta_2 - \theta_1\cosh M\beta_a)\sinh M\beta/\sinh M\beta_a \tag{18}$$

$$\bar{m}(\beta) \equiv \frac{m(y)}{Q/h_{fg}} = \frac{L}{L_e}\int_0^\beta \theta_a(\beta)\, d\beta =$$

$$\frac{1}{\eta_e}\left[\theta_1\frac{\sinh M\beta}{M} + (\theta_2 - \theta_1\cosh M\beta_a)\frac{(\cosh M\beta - 1)}{M\sinh M\beta_a}\right] \tag{19}$$

It should be noted that $m(y)$ is the net mass flow rate calculated from the junction of the heat input and adiabatic sections to some location y in the adiabatic section. For the actual mass flow in the adiabatic section, $m(y)$ should be added by the mass flow generated in the heat input section $m(L_e)$.

Combining Eqs. (14, 16, and 18) with Eq. (10), there result the following expressions for θ_1 and θ_2:

$$\theta_1 = (1/\alpha)\{Bi\theta_0\,\gamma_2/(1+Bi)^{1/2} + \gamma_1[\gamma_2\gamma_3(1+Bi)^{1/2} + \gamma_4]\} \tag{20}$$

and

$$\theta_2 = \theta_1(\gamma_1\gamma_3 + \gamma_4) - \gamma_1\gamma_3 \tag{21}$$

where

$$\gamma_1 \equiv \tanh M\eta_e, \qquad \gamma_2 \equiv \tanh M(1+Bi)^{1/2}\xi_c$$

$$\gamma_3 \equiv \sinh M\beta_a, \qquad \gamma_4 \equiv \cosh M\beta_a$$

$$\alpha \equiv (1+Bi)^{1/2}(\gamma_1\gamma_2\gamma_3 + \gamma_2\gamma_4) + \gamma_1\gamma_4 + \gamma_3$$

Combining the enclosure condition, Eq. (13) with Eqs. (16, 20, and 21), gives the expression for θ_0

$$\theta_0 = \frac{-\eta_e\alpha/Bi + \gamma_1\gamma_2/M(1+Bi)^{1/2}}{\xi_c\alpha/(1+Bi) + Bi(\gamma_1\gamma_2\gamma_4 + \gamma_2\gamma_3)/M(1+Bi)^{3/2}} \tag{22}$$

or in the functional form

$$\theta_0 = \theta_0(\eta_e, \beta_a, \xi_c, M, Bi) \tag{23}$$

With known values of the dimensionless parameters which appear in Eq. (23), θ_0 can be calculated without difficulty and thus, T_s is known. Substituting the value of θ_0 into Eqs. (20) and (21) determines θ_1 and θ_2. With θ_0, θ_1 and θ_2 known, the dimensionless wall temperature and mass flow distributions can be calculated.

For the case of heat pipes operating with two constant temperature surroundings, the heat-transfer rate is not known; the normalizing factors for the dimensionless wall temperature and mass flow rate are different from the previous case of heat pipes with uniform heat addition to the heat input section. Solutions can be obtained simply by following the same steps in the previous analysis. The results and discussions are given in the Appendix.

Results and Discussions

The dimensionless parameters which appeared in the theoretical analysis consist of the dimensionless length (η), temperature (θ), and mass flow rate ($\bar{m}$), as well as Bi and M. The last two parameters play a significant role on the heat pipe performance and their physical meaning merits further discussion. The Biot number with respect to wick Bi characterizes the relative magnitude of the radial temperature drop in the wick with that between pipe wall and its outside surroundings. For large Bi, the mechanism of heat rejection is very effective compared to the radial conduction through wick, and consequently, the temperature difference between the wall and the ambient is very small compared to that between the wall and vapor. Conversely, for very small Bi, the temperature difference in the wick is negligible compared to that between the wall and the ambient. The typical values of Bi are on the order between 10^{-4} and 10^{-1} for heat pipes operating with heat rejection by free convection or by radiation, between 10^{-1} and 10 for those with heat exchanger for heat removing, and between 1 and 10^3 for those with boiling as the heat removing mechanism.

The physical meaning of M, which is defined in Eq. (4), becomes clear in the limiting case when the pipe diameter is much larger than the wall and wick thickness. In this case, M can be reduced to

$$M = [(k_i/t_i)/(k_w/t_w)]^{1/2}[L/t_w] \tag{24}$$

The first bracketed term is the comparison of wick conductance with wall conductance, while the second term represents the relative magnitude of the surface area of the pipe to the cross-sectional area of the wall. With the increase of M, more heat will be transferred radially through the larger surface area with less resistance than that transferred axially through the small cross-sectional area of the wall. Theoretically, $M \to \infty$ represents the case of no axial heat conduction. The typical values of M, for existing heat pipes, range from the order of 10^3 to 10.

The dimensionless saturated vapor temperature θ_0 as given in Eq. (22), is shown in Fig. 2 as a function of Bi and M for a set of fixed values of η_e, ξ_c and β_a. It shows that θ_0 is strongly dependent on Bi, especially for small Bi. In the limit $Bi \to 0$, all the curves of different M converge to a single straight line, and Eq. (22) reduces to

$$\lim_{Bi\to 0}[-\theta_0] = \eta_e/\xi_c Bi \tag{25}$$

or

$$Q = \pi D_0 L_c h(T_s - T_0) \tag{26}$$

This means physically that the temperature difference between the wall and vapor at small Bi is so small as compared to that between the wall and the ambient, that the heat pipe appears as being isothermal at the vapor temperature T_s with respect to the ambient temperature T_0.

As Bi increases, θ_0 becomes less dependent on Bi. For Bi approaches infinity, θ_0 is completely determined by the heat pipe geometry and M. By taking the limiting condition of Eq. (22), there follows

$$\lim_{Bi\to\infty}[-\theta_0] = \frac{\eta_e - \gamma_1/M(\gamma_1\gamma_3+\gamma_4)}{\xi_c+(\gamma_1\gamma_4+\gamma_3)/M(\gamma_1\gamma_3+\gamma_4)} \tag{27}$$

For the case of $M \to \infty$, Eq. (27) reduces to

$$\lim_{\substack{Bi\to\infty \\ M\to\infty}}[-\theta_0] = \eta_e/\xi_c \tag{28}$$

or

$$Q = 2\pi L_c k_i (T_s - T_0)/\ln D_i/D_v \tag{29}$$

This implies that for a heat pipe with no axial conduction, the wall temperature in the heat output section is equal to the ambient temperature when $Bi \to \infty$, and the heat rejection is uniform along the pipe.

The values of η_e, β_a and ξ_c used in Fig. 2 are arbitrarily chosen. By varying η_e, β_a and ξ_c, the results can become substantially different. For instance, the asymptote ($Bi \to \infty$) for the case of $\eta_e = \frac{1}{6}$, $\xi_c = \frac{5}{6}$ and $\beta_a = 0$ as shown by the dotted line differs appreciably from the asymptote of the solid lines. This indicates that by removing the insulation which originally covers three-sixths of the heat pipe, and extending the heat output section to five-sixths of the total length under the same ambient condition, the dimensionless saturated vapor temperature is reduced to two-fifths of its original value.

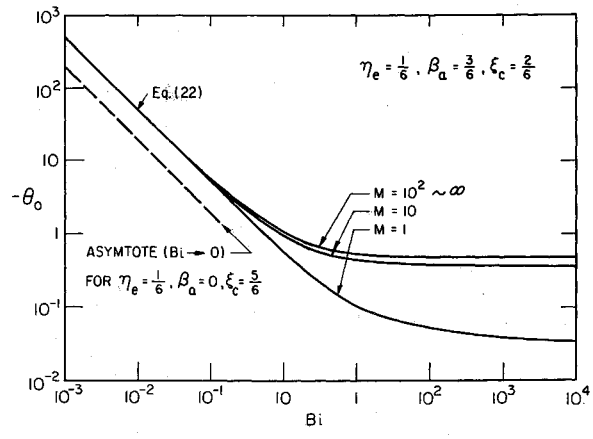

Fig. 2 Variation of θ_0 with Bi and M.

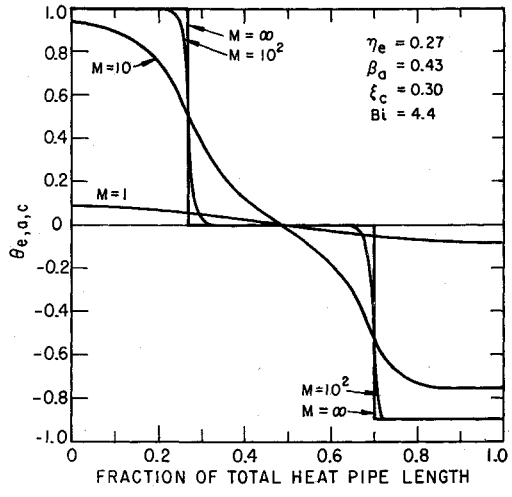

Fig. 3 Variation of the dimensionless axial wall temperature with M.

Figure 3 depicts the variation of the dimensionless wall temperature calculated from Eqs. (14, 16, and 18) with M for an arbitrarily chosen heat pipe geometry (i.e., η_e, β_a, ξ_c) and a specific value Bi. The effect of axial conduction on the thermal performance is manifest. For $M \to \infty$, the case of no axial heat conduction, the wall temperatures are uniform in the heat input and output sections, and equal to the vapor temperature in the adiabatic section. For $M = 10^2$, the wall temperature profile near the junctions of heat pipe sections deviates slightly from the straight lines, indicating the effect of axial conduction. For $M = 10$ and $M = 1$, the effect of axial conduction is more pronounced. It is shown that, even with 43% of the pipe insulated, axial conduction causes the isothermal region to be nonexistent. Figure 3 also indicates that axial heat conduction through the wall actually reduces the total temperature drop between the two ends of the heat pipe, in contrast with the widely accepted notion of reducing wall conduction in order to minimize the total temperature drop.

The axial mass flow distributions corresponding to the wall temperature profiles given in Fig. 3 are calculated from Eqs. (15, 17, and 19), and presented in Fig. 4. For $M \to \infty$, the dimensionless axial mass flow varies linearly in the heat input and output sections, while remaining constant at unity in the adiabatic section. This represents uniform blowing (evaporation) in the heat input section and uniform suction (condensation) in the heat output section. In this case, the heat input and output sections are

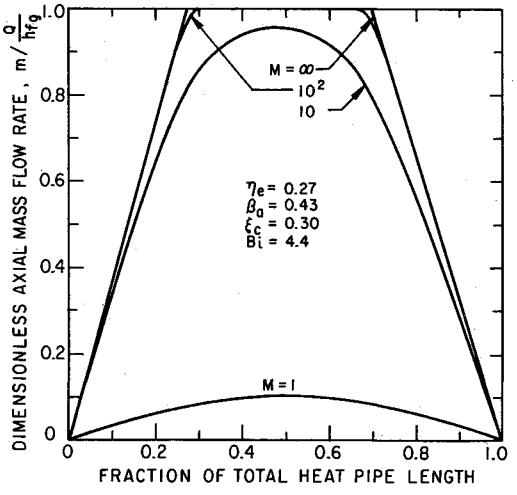

Fig. 4 Variation of the dimensionless axial mass flow rate with M.

identical with the effective evaporator and condenser. For $M = 10^2$, while axial conduction has lengthened slightly the vaporization and condensation regions, all the heat input is still preserved by the adiabatic section. For $M = 10$, only 95.5% of heat input takes part in the evaporation and condensation processes, while the rest is transferred directly to the ambient. For $M = 1$, axial conduction is so predominant that 89.9% of the heat input bypasses the vapor zone. At a certain location on the length (horizontal) coordinate in Fig. 4, the vertical distance between the curve of a certain M value and the curve of $M \to \infty$ indicates the amount of axial conduction at that location in percentage of heat input. It is obvious that, for heat pipes designed with M of the order of 10 or less, the effect of axial conduction cannot be neglected.

Consider now the comparison of the present predictions with existing experimental results of heat-pipe performance. Reported experimental investigations contain little information on the mass flow distribution in a heat pipe, but some results are available on the saturated vapor temperature and wall temperature distributions, which could be used for comparison. To have a direct comparison, however, requires accurate data on the following system variables: the rate of heat input Q, the ambient temperature T_0, the heat pipe geometry (L_e, L_a, L_c, D_0, D_i and D_v), the conductivities k_w and k_i, and the heat-transfer coefficient h. The precise values of some of these parameters in many experiments are difficult to determine or to estimate, particularly the values of h and k_i. Indeed, the saturated vapor temperature is rather sensitive to the variation of h, especially when $Bi \ll 1$, while the wall temperature distribution depends strongly on k_i. The assumption of constant k_i is somewhat controversial.[1] This is largely due to the uncertainties of meniscus receding, vapor generation and vapor trap in the wick. Generally speaking, for heat flux not very close to the operational limits, this assumption appears quite reasonable. Moreover, in existing experimental investigations with detailed measurements of saturated vapor temperature and wall temperature distributions,[4-7] a meaningful comparison cannot always be established because of the fact that some key information is missing. For instance, the ambient temperature in one reported investigation[4] was not given, while for heat pipe operating in a vertical position[5] or charged with excessive working fluid,[5,6] there exists great uncertainty in the thickness and uniformity of the wick liquid matrix.

Figure 5 shows the comparison of predicted axial wall temperature profile with the experimental data of Holm and Miller,[7] which were obtained under different levels of heat input. The h values used in the comparison are determined from experimental results by using Newton's cooling law,

$$Q = \pi D_0 L_c h(\bar{T}_{wc} - T_0)$$

The effective thermal conductivity of the liquid-wick matrix k_i is not known, but based on the current experimental evidence,[8] the

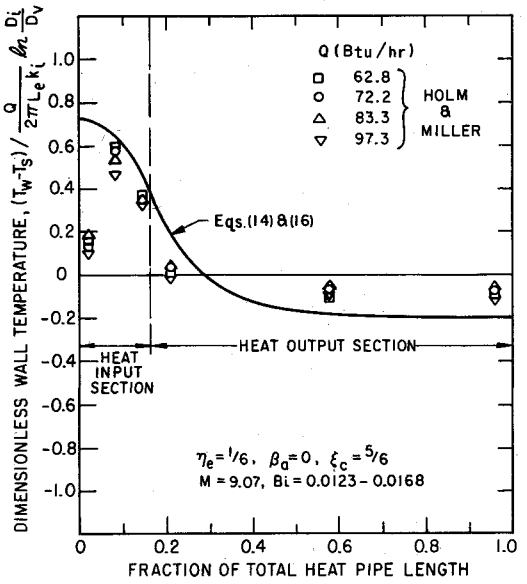

Fig. 5 Comparison of predicted axial wall temperature profile with experimental data.

value of k_i for screen wicks can be well approximated by assuming the composed phases arranged in series. The Bi values in these cases vary from 0.0123 to 0.0168, which makes negligible difference on the plot of dimensionless wall temperature profiles. It is shown that the experimental data not only correlate well in the appropriate dimensionless form, but also agree well with the theoretical prediction. This demonstrates that the effect of axial conduction is indeed appreciable in the case of M equal to 9.07. Indeed, the present prediction shows that about 38% of the total heat input is transferred axially across the junction of heat input and heat output sections. The deviation of experimental data near the ends of heat pipe is evidently due to heat loss through the end caps. Another possible course of error is, of course, due to the inaccurate k_i value used in the calculation. It should be pointed out, however, that one set of Holm and Miller's data (from the prototype heat pipe) cannot be correlated with the present prediction. The exact cause of this discrepancy is difficult to ascertain, but this particular set of data does indicate a predominant effect of axial wall conduction.

A final remark seems in order as a result of the present study. In the existing literature, it is very popular to analyse the heat transfer characteristics of wicks through the well-known $q - \Delta T$ relation.[1] This is based on the assumption that axial conduction is negligible, and the wall temperature is constant. For heat pipes with small values of M, however, this is not a meaningful representation.

Summary and Conclusions

The steady-state performance of a single component heat pipe can be well explained by a simple conduction model with an enclosure condition. The conduction model deals with the local wall temperature and mass flow rate, while the enclosure condition based on the over-all energy and mass continuity determines the saturated vapor temperature, i.e., the mean temperature of the heat pipe.

The results obtained in the present analysis lead to several conclusions and design implications.

1) The phase change phenomena inside the heat pipe is to maintain a near uniform condition in the vapor region. It does not exert noticeable influence on the steady-state wall temperature distribution and saturated vapor temperature. For a constant heat input, however, the mass flow rate is inversely proportional to the latent heat of the phase change.

2) In addition to the dependence on heat pipe geometries, the thermal performance of a heat pipe can be greatly influenced by two dimensionless parameters, Bi and M. The parameter Bi

characterizes the heat removing mechanism at the ambient, while M governs the effect of axial conduction along wall. Axial conduction becomes more predominant at smaller values of M. For a fixed heat load, the vapor temperature inside the pipe always decreases as the external condenser heat-transfer coefficient increases. However, for a constant external surrounding (or surroundings) and wick conductance, the increase in axial conduction results in a decrease of the vapor temperature for the case of heat pipes operating with uniform heat input but an increase for the case of heat pipes operating in two constant temperature zones.

3) The thermal behavior of heat pipes can be considered as heat flow from the source to the sink through a series of thermal resistance. For a fixed heat pipe geometry, the wick resistance decreases with M. Thus, for the case of heat pipes operating with uniform heat input, the over-all temperature drop decreases with M. And, for the case of heat pipes operating in two constant temperature zones, the heat transfer capacity increases as M decreases. In other words, the thermal effectiveness and the capacity of heat transport of the heat pipe can be increased by increasing axial conduction through wall.

4) One of the design criteria for heat pipes is the maximum capacity of heat transport which is often limited by wick capillary pumping. Since the mass flow rate decreases with M, it is possible to increase the maximum heat transport capacity by increasing axial conduction through wall.

5) An optimized heat pipe design can be achieved with the smallest allowable M value. That means to maximize axial conduction along wall, which can be made by increasing the wall conductance or wall thickness in some cases, under certain specific design constraints.

Appendix

The solutions are obtained for the thermal performance of heat pipes operating in two constant temperature surroundings, with temperature T_λ and heat-transfer coefficient h_λ in the warm surroundings (source), and T_0, h_0 in cold ambient (sink).

Wall Temperature

For $0 \leqq \eta \leqq \eta_e$

$$\theta_e(\eta) \equiv [T_{we}(x) - T_0]/[T_\lambda - T_0] = \frac{B_\lambda + \theta_s}{1+B_\lambda} + \left(\theta_1 - \frac{B_\lambda+\theta_s}{1+B_\lambda}\right)\frac{\cosh M(1+B_\lambda)^{1/2}\eta}{\cosh M(1+B_\lambda)^{1/2}\eta_e} \quad \text{(A1)}$$

For $0 \leqq \beta \leqq \beta_a$

$$\theta_a(\beta) \equiv [T_{wa}(y) - T_0]/[T_\lambda - T_0] = \theta_s + (\theta_1 - \theta_s)\cosh M\beta + [(\theta_2 - \theta_s) - (\theta_1 - \theta_s)\cosh M\beta_a]\sinh M\beta/\sinh M\beta_a \quad \text{(A2)}$$

For $0 \leqq \xi \leqq \xi_c$

$$\theta_c(\xi) \equiv [T_{wc}(z) - T_0]/[T_\lambda - T_0] = \theta_s/(1+B_0) + [\theta_2 - \theta_s/(1+B_0)]\cosh M(1+B_0)^{1/2}\xi/\cosh M(1+B_0)^{1/2}\xi_c \quad \text{(A3)}$$

Mass Flow Rate

For $0 \leqq \eta \leqq \eta_e$

$$\bar{m}(\eta) \equiv \frac{m(x)}{2\pi k_i L(T_\lambda - T_0)/h_{fg}\ln Di/D_v} = \frac{B_\lambda(1-\theta_s)\eta}{1+B_\lambda} + \frac{\left(\theta_1 - \dfrac{B_\lambda+\theta_s}{1+B_\lambda}\right)}{M(1+B_\lambda)^{1/2}}\frac{\sinh M(1+B_\lambda)^{1/2}\eta}{\cosh M(1+B_\lambda)^{1/2}\eta_e} \quad \text{(A4)}$$

For $0 \leqq \beta \leqq \beta_a$

$$\bar{m}(\beta) \equiv \frac{m(y)}{2\pi k_i L(T_\lambda - T_0)/h_{fg}\ln D_i/D_v} = (\theta_1 - \theta_s)\sinh M\beta/M + [(\theta_2 - \theta_s) - (\theta_1 - \theta_s)\cosh M\beta_a](\cosh M\beta - 1)/M\sinh M\beta_a \quad \text{(A5)}$$

For $0 \leqq \xi \leqq \xi_c$

$$\bar{m}(\xi) \equiv \frac{m(z)}{2\pi k_i L(T_\lambda - T_0)/h_{fg}\ln D_i/D_v} = \frac{(\theta_s B_0)\xi}{1+B_0} - \frac{[\theta_2 - \theta_s/(1+B_0)]}{M(1+B_0)^{1/2}}\frac{\sinh M(1+B_0)^{1/2}\xi}{\cosh M(1+B_0)^{1/2}\xi_c} \quad \text{(A6)}$$

Heat Flux through the Pipe

$$\frac{Q}{2\pi k_i L(T_\lambda - T_0)/\ln D_i/D_v} = \frac{B_0\theta_s\xi_c}{1+B_0} + \frac{\gamma_2 B_0[\theta_2 - \theta_s/(1+B_0)]}{M(1+B_0)^{1/2}} \quad \text{(A7)}$$

where

$$\theta_s \equiv \frac{T_s - T_0}{T_\lambda - T_0} = \frac{[\gamma_1\delta_2(1+B_\lambda)^{1/2} + \delta_1]\dfrac{B_\lambda\eta_e}{1+B_\lambda} + \dfrac{\delta_1\gamma_1 B_\lambda^{\,2}}{M(1+B_\lambda)^{3/2}} - \dfrac{\gamma_1\gamma_2 B_0 B_\lambda}{M(1+B_0)^{1/2}(1+B_\lambda)^{1/2}}}{[\gamma_1\delta_2(1+B_\lambda)^{1/2} + \delta_1]\left(\dfrac{B_\lambda\eta_e}{1+B_\lambda} + \dfrac{B_0\xi_c}{1+B_0}\right) + \dfrac{\delta_1\gamma_1 B^{\lambda 2}}{M(1+B_\lambda)^{3/2}} + \dfrac{\delta_3\gamma_2 B_0^{\,2}}{M(1+B_0)^{3/2}} - \dfrac{2\gamma_1\gamma_2 B_0 B_\lambda}{M(1+B_0)^{1/2}(1+B_\lambda)^{1/2}}} \quad \text{(A8)}$$

and

$$\theta_1 = \frac{T_{w1} - T_0}{T_\lambda - T_0} = \frac{\theta_s[\delta_1 + \delta_2\gamma_1/(1+B_\lambda)^{1/2} - \gamma_2 B_0/(1+B_0)^{1/2}] + \gamma_1\delta_2 B_\lambda/(1+B_\lambda)^{1/2}}{\gamma_1\delta_2(1+B_\lambda)^{1/2} + \delta_1} \quad \text{(A9)}$$

$$\theta_2 = \frac{T_{w2} - T_0}{T_\lambda - T_0} = \frac{\theta_s[\delta_3 + \delta_4\gamma_2/(1+B_0)^{1/2} - \gamma_1 B_\lambda/(1+B_\lambda)^{1/2}] + \gamma_1 B_\lambda/(1+B_\lambda)^{1/2}}{\gamma_1\delta_2(1+B_\lambda)^{1/2} + \delta_1} \quad \text{(A10)}$$

$$B_\lambda \equiv (h_\lambda D_0/2k_i)\ln D_i/D_v, \quad B_0 = (h_0 D_0/2k_i)\ln(D_i/D_v) \quad \text{(A11)}$$

$$\gamma_1 \equiv \tanh M(1+B_\lambda)^{1/2}\eta_e, \quad \gamma_2 \equiv \tanh M(1+B_0)^{1/2}\xi_c,$$
$$\gamma_3 \equiv \sinh M\beta_a, \quad \gamma_4 \equiv \cosh M\beta_a$$
$$\delta_1 \equiv \gamma_3 + \gamma_2\gamma_4(1+B_0)^{1/2}, \quad \delta_2 \equiv \gamma_4 + \gamma_2\gamma_3(1+B_0)^{1/2}$$
$$\delta_3 \equiv \gamma_3 + \gamma_1\gamma_4(1+B_\lambda)^{1/2}, \quad \delta_4 \equiv \gamma_4 + \gamma_1\gamma_3(1+B_\lambda)^{1/2}$$

It should be noted that there are six independent dimensionless parameters—with one additional Biot number with respect to the wick. In this case, the saturated vapor temperature increases as M decreases, instead of decreasing with M in the previous case shown in Fig. 2. This is due to the fact that axial conduction through the wall spreads the influence of high temperature zone. This is the major difference in the performance characteristics from the previous case of heat pipes operating with uniform heat input. The dependence of the dimensionless wall temperature and axial mass flow rate on M for fixed Biot numbers and geometric parameters is similar to the previous results as presented in Figs. 3 and 4. Since the heat input is not given in this case, it is of particular interest to determine the heat transport through a heat pipe under prescribed source and sink conditions. For a special case when two end portions of a heat pipe are in contact with solid bodies at different temperatures with negligible contact resistance, the Biot numbers, B_λ and B_0, approach infinity. The variation of the dimensionless heat flux with M for arbitrarily fixed values of η_e, β_a and ξ_c is

given in Fig. 6. It is shown that by increasing axial conduction, the energy transferred through a heat pipe can be increased substantially.

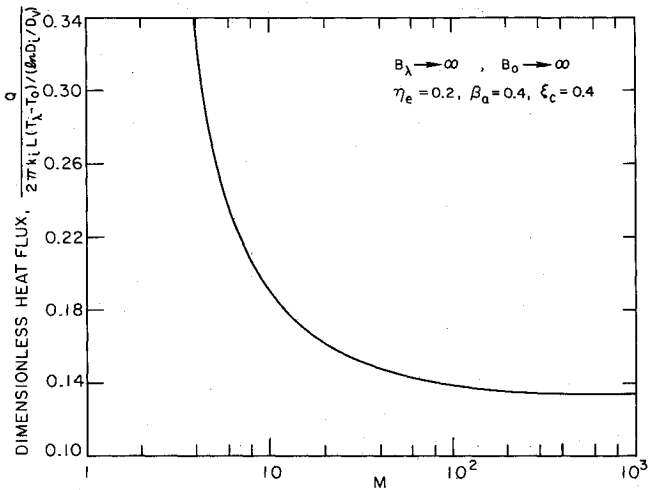

Fig. 6 Variation of the dimensionless heat flux with M.

References

[1] Winter, E. R. F. and Barsch, W. O., "The Heat Pipe," *Advances in Heat Transfer,* edited by T. F. Irvine and J. P. Hartnett, Vol. 7, Academic Press, New York, 1971, pp. 219–320.

[2] Edwards, D. K. and Marcus, B. D., "Heat and Mass Transfer in the Vicinity of the Vapor-Gas Front in a Gas Loaded Heat Pipe," Paper 71-WA/HT-29, 1971, ASME.

[3] Marcus, B. D., "Theory and Design of Variable Conductance Heat Pipes: Hydrodynamics and Heat Transfer," Research Rept. 1, April 1971, TRW Systems Group, Redondo Beach, Calif.

[4] Schwartz, J., "Performance Map of the Water Heat Pipe and the Phenomenon of Non-condensible Gas Generation," Paper 69-HT-15, 1969, ASME.

[5] Tien, C. L., "Two-Component Heat Pipes," *Progress in Astronautics and Aeronautics,* edited by J. T. Bevans, Vol. 23, Academic Press, New York, 1970, pp. 423–436.

[6] Tien, C. L. and Rohani, A. R., "Theory of Two-Component Heat Pipes," Paper 71-WA/HT-30, 1971, ASME.

[7] Holm, F. W. and Miller, P. L., "Thermal Scale Modeling of a Heat Pipe," Paper 70-HT/SpT-14, 1970, ASME.

[8] Seban, R. A. and Abhat, A., "Steady and Maximum Evaporation from Screen Wicks," Paper 71-WA/HT-12, 1971, ASME.